Probing the neutron skin variations in isotope pairs by hyperon-antihyperon production in antiproton–nucleus interactions

Falk Schupp[a], Josef Pochodzalla[a,b,*], Patrick Achenbach[a,b,1], Michael Bölting[a], Martin Christiansen[a], Theodoros Gaitanos[c], Horst Lenske[d], Marcell Steinen[a]

[a] *Helmholtz Institute Mainz, GSI Helmholtz Centre for Heavy Ion Research, Darmstadt, Johannes Gutenberg University, 55099 Mainz, Germany*
[b] *Institute for Nuclear Physics, Johannes Gutenberg University, 55099 Mainz, Germany*
[c] *Department of Theoretical Physics, Aristotle University of Thessaloniki, GR-54124 Thessaloniki, Greece*
[d] *Institut für Theoretische Physik, Justus-Liebig-Universität Gießen, D-35392 Gießen, Germany*

- Motivation
- Neutron skin
- Method
- Remarks on feasibility

Mass – Radius Relation

- Stellar matter in hydrostatic equlibrium
- Described by GR and Tolman–Oppenheimer–Volkoff (TOV) equation

$$\frac{dP}{dr} = -\frac{G \cdot M(r) \cdot \varepsilon(P)}{r^2 c^2} \cdot \left(1 + \frac{P}{\varepsilon(P)}\right) \cdot \left(1 + \frac{4\pi r^3 P}{M(r) \cdot c^2}\right)\left(1 - \frac{2GM(r)}{rc^2}\right)^{-1}$$

  - P: pressure
  - ε: energy density
  - M(r): mass enclosed within radius r

$$\frac{dM(r) \cdot c^2}{dr} = 4\pi r^2 \varepsilon(P)$$

- Specific solution (M,R) requires Equation of state ε(P) as input
  - Soft EoS: low maximum mass and small radii
  - Stiff EoS: high maximum mass and large radii

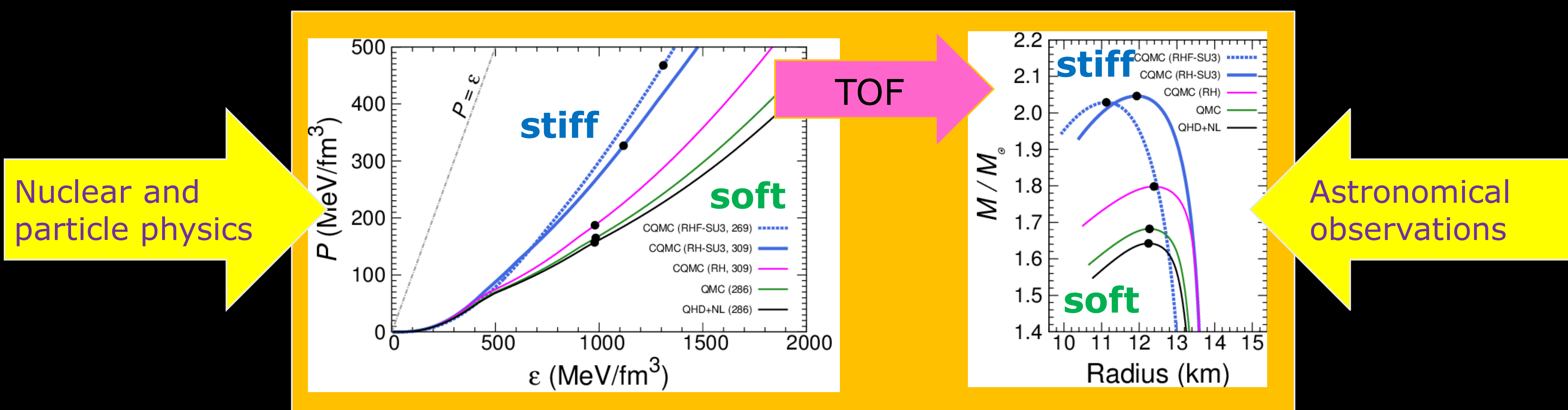

Nuclear Equation of State

- Approximated by Taylor expansion around normal nuclear density ρ_0

isoscalar part E_{SNM} | isovector part E_{sym}

$$E(\rho,\delta) = E_0 + \frac{K_0}{2}\cdot\left(\frac{\rho-\rho_0}{3\rho_0}\right)^2 + \left[S_0 + L\cdot\left(\frac{\rho-\rho_0}{3\rho_0}\right) + \frac{K_{sym}}{2}\cdot\left(\frac{\rho-\rho_0}{3\rho_0}\right)^2\right]\cdot\delta^2$$

incompressibility $K_0 = 9\rho_0^2 \frac{d^2E_{SNM}}{d\rho^2}(\rho_0)$

symmetry energy $S_0 = \frac{1}{2}\frac{\partial^2 E}{\partial\delta^2}(\rho_0, 0)$

slope of E_{sym} $L = 3\rho_0 \frac{dE_{sym}}{d\rho}(\rho_0)$

$K_{sym} = 9\rho_0^2 \frac{d^2E_{sym}}{d\rho^2}(\rho_0)$

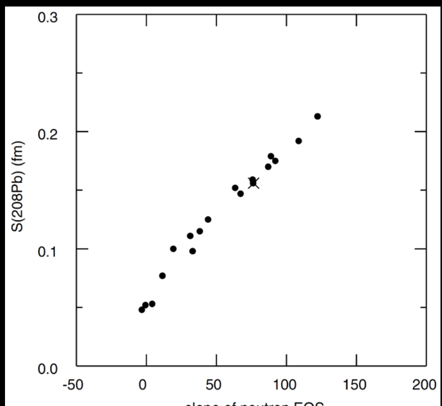

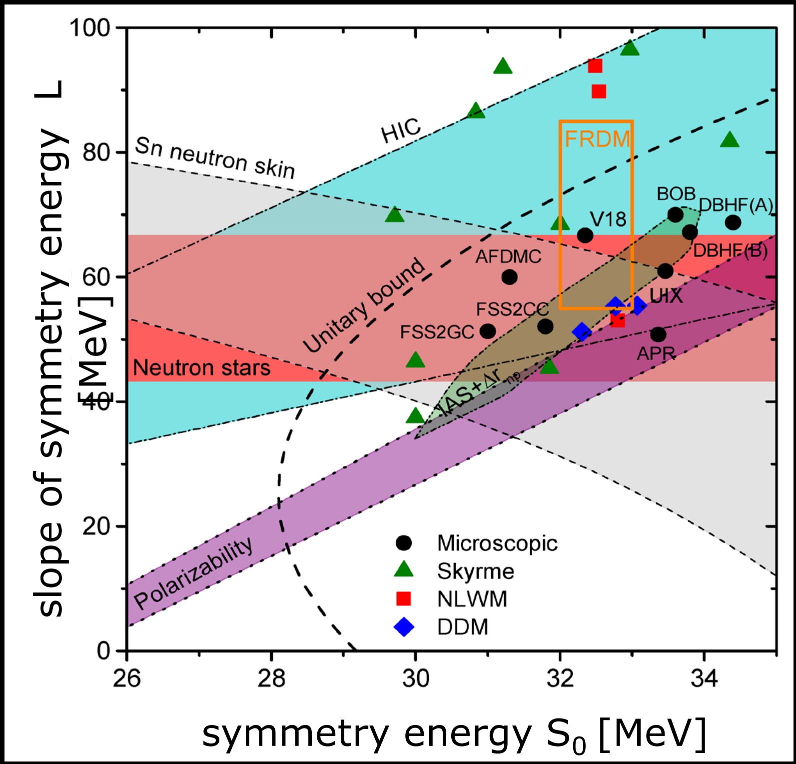

Nuclear Physics with $\bar{p}$+A interactions

neutron skin
anihyperons in nuclei
hyper- and antihyper atoms
double hypernuclei

$\bar{\Lambda}\Lambda$ and $\bar{\Lambda}\Sigma$
$\bar{\Lambda}\Lambda$
tagged negativ (anti)hyperons
tagged Ξ

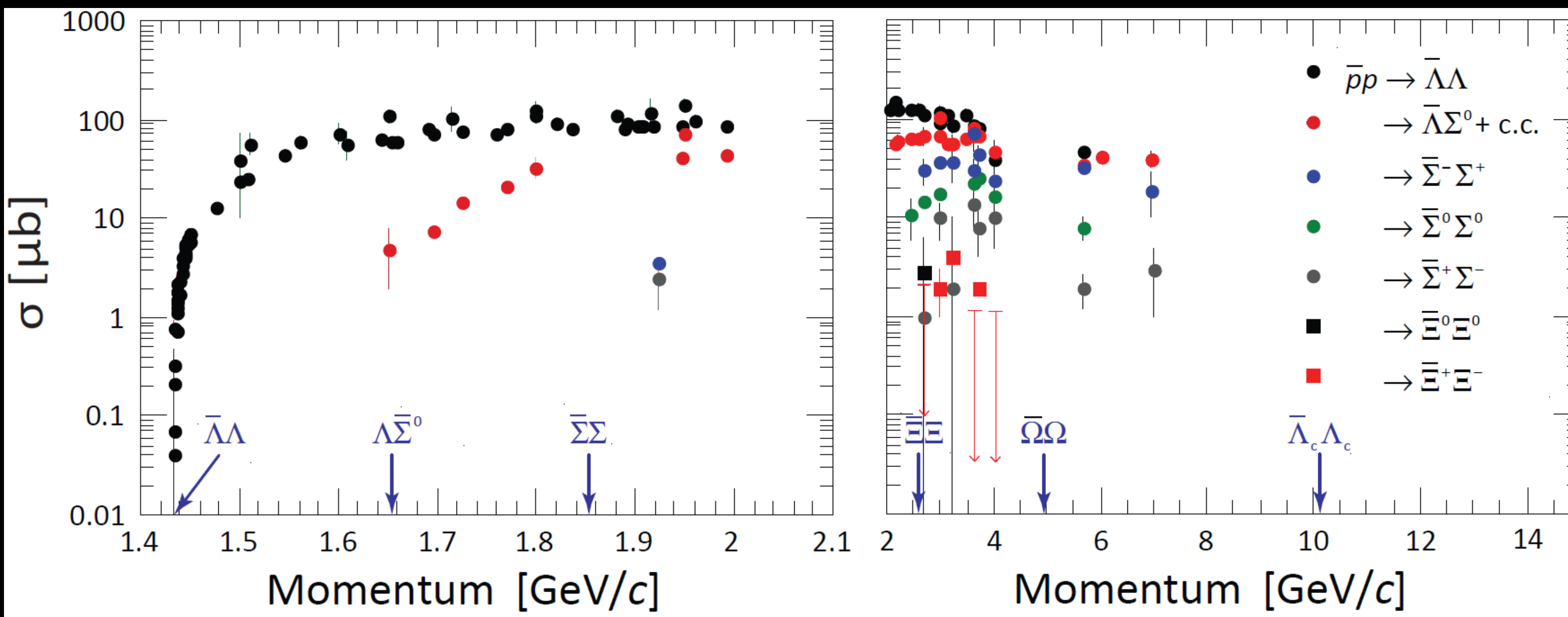

Neutron skin

- Neutron skin defined as $R_{rms}(n)$ - $R_{rms}(p)$
- Definition of neutron skins is not unique

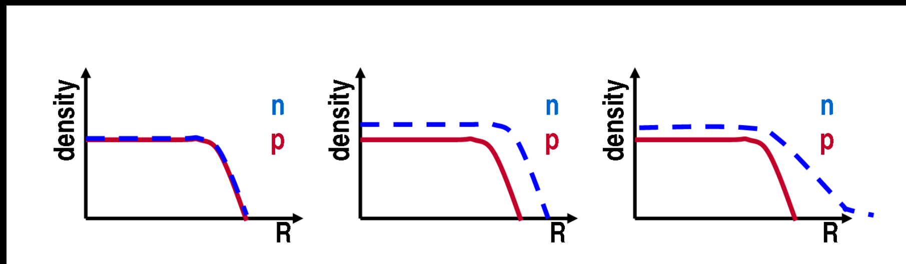

M Thiel et al 2019 J. Phys. G: Nucl. Part. Phys. 46 093003

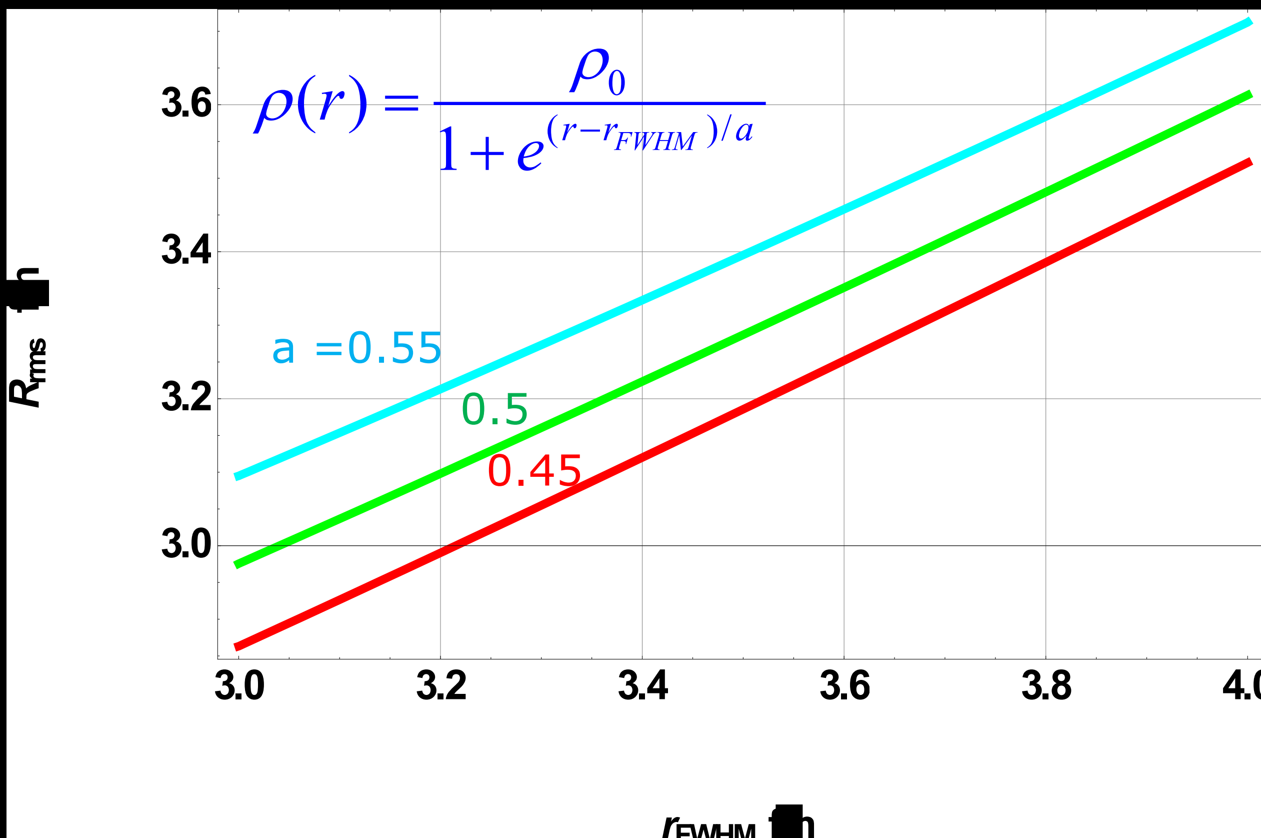

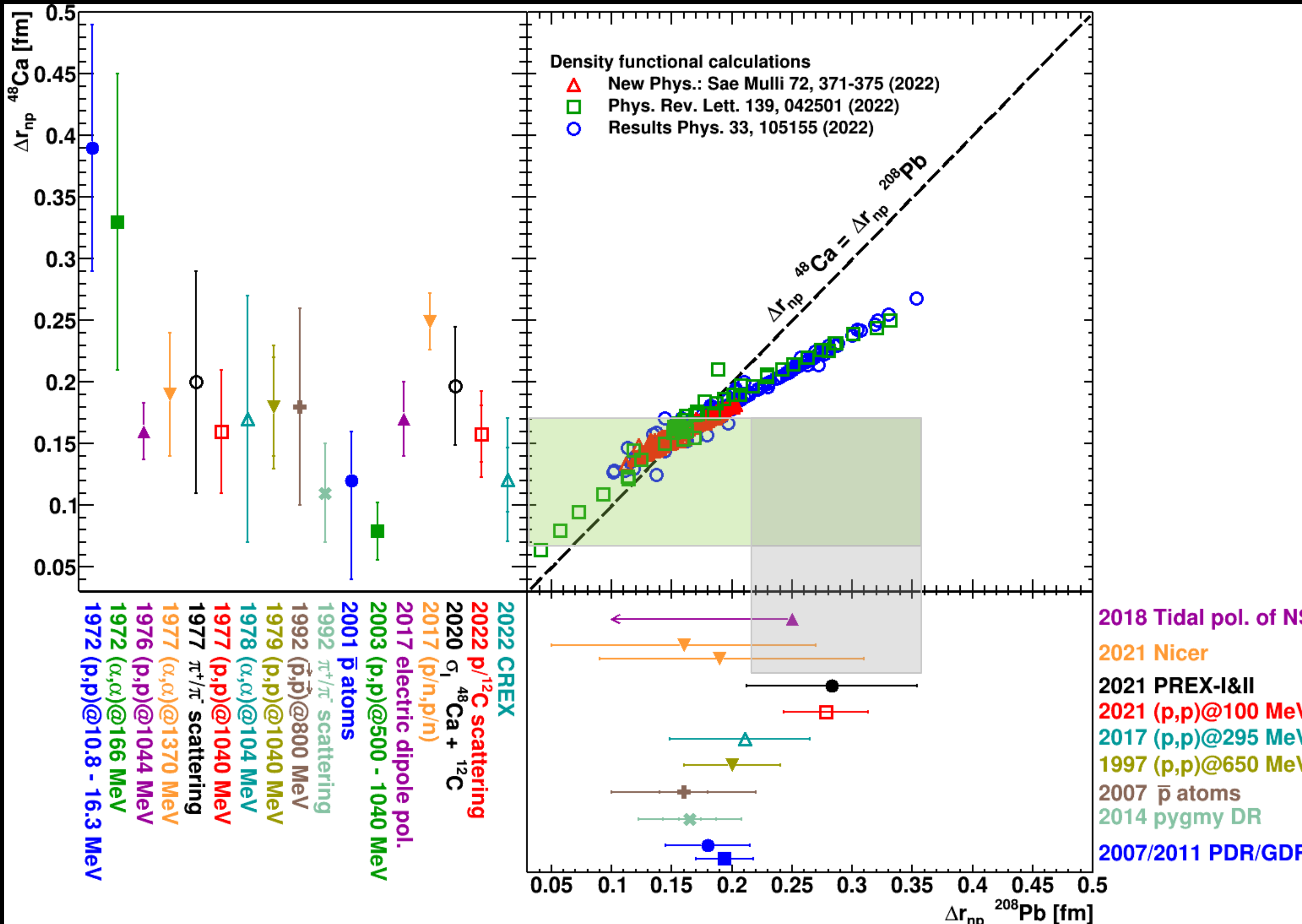

Density functional calculations
New Phys.: Sae Mulli 72, 371-375 (2022)
Phys. Rev. Lett. 139, 042501 (2022)
Results Phys. 33, 105155 (2022)
Δr_{np} ^{48}Ca = Δr_{np} ^{208}Pb
Δr_{np} ^{48}Ca [fm]
Δr_{np} ^{208}Pb [fm]
1972 (p,p)@10.8 - 16.3 MeV
1972 (α,α)@166 MeV
1976 (p,p)@1044 MeV
1977 (α,α)@1370 MeV
1977 π+/π- scattering
1977 (p,p)@1040 MeV
1978 (α,α)@104 MeV
1979 (p,p)@1040 MeV
1992 (p,p)@800 MeV
1992 π+/π- scattering
2001 p̄ atoms
2003 (p,p)@500 - 1040 MeV
2017 electric dipole pol.
2017 (p/n,p/n)
2020 σI 48Ca + 12C
2022 p/12C scattering
2022 CREX
2018 Tidal pol. of NS
2021 Nicer
2021 PREX-I&II
2021 (p,p)@100 MeV
2017 (p,p)@295 MeV
1997 (p,p)@650 MeV
2007 p̄ atoms
2014 pygmy DR
2007/2011 PDR/GDR

Idea

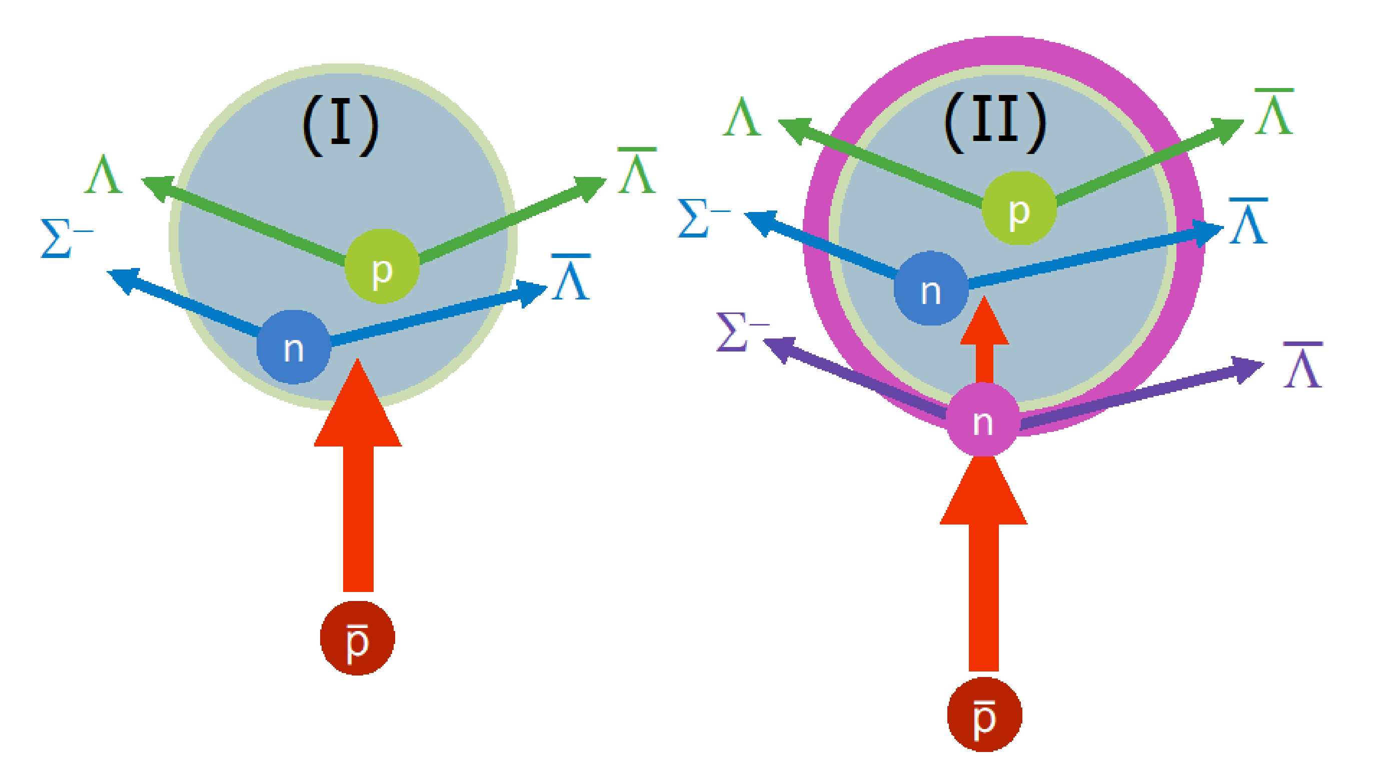

$$DR = \frac{p^a_{\Sigma^-\bar{\Lambda}} / p^a_{\Lambda\bar{\Lambda}}}{p^b_{\Sigma^-\bar{\Lambda}} / p^b_{\Lambda\bar{\Lambda}}} \approx \frac{1+p_{abs}}{1-p_{abs}}$$

$$\text{with} \quad p_{abs} = 1-\exp\left(-\sigma_{\bar{p}n} \cdot \int_{\Delta_n} \rho_n \cdot dr_n\right)$$

arXiv:2209.03875

Studied isotope pairs

isotope	abundance [%]	exp. proton radius R_p^{exp} [fm]	proton radius R_p [fm]	neutron radius R_n [fm]	neutron skin ΔR_{pn} [fm]	skin difference Δ_n [fm]	RMF model
^{20}Ne	90.5	2.992±0.008 [51]	2.782	2.758	-0.024	–	NL3 [52]
^{22}Ne	9.3	2.986±0.021 [51]	2.800	2.887	0.087	0.111	NL3 [52]
^{40}Ca	96.9	3.4776±0.0019 [53]	3.452	3.416	-0.036		NL1 [52]
^{48}Ca	0.187	3.4786±0.0106 [53, 54]	3.525	3.731	0.206	0.242	NL1 [52]
^{40}Ca	96.9	3.4776±0.0019 [53]	3.391	3.354	-0.037	–	NL3 [52]
^{48}Ca	0.187	3.4786±0.0106 [53, 54]	3.472	3.659	0.187	0.224	NL3 [52]
^{40}Ca	96.9	3.4776±0.0019 [53]	3.396	3.360	-0.036	–	NL3* [55]
^{48}Ca	0.187	3.4786±0.0106 [53, 54]	3.475	3.666	0.191	0.227	NL3* [55]
^{40}Ca	96.9	3.4776±0.0019 [53]	3.117	3.090	-0.028	–	Set I [56]
^{48}Ca	0.187	3.4786±0.0106 [53, 54]	3.243	3.357	0.1114	0.142	Set I [56]
^{58}Ni	68.1	3.770±0.002 [57]	3.769	3.768	0.000	–	NL3 [52]
^{64}Ni	0.926	3.854±0.002 [57]	3.822	3.947	0.125	0.125	NL3 [52]
^{129}Xe	26.4	4.7775±0.0050 [53]	4.768	4.932	0.164	–	NL3 [52]
^{130}Xe	4.1	4.7818±0.0049 [53]	4.776	4.950	0.174	0.010	NL3 [52]
^{131}Xe	21.2	4.7808±0.0049 [53]	4.784	4.968	0.184	0.020	NL3 [52]
^{132}Xe	26.9	4.7859±0.0048 [53]	4.792	4.986	0.194	0.030	NL3 [52]
^{134}Xe	10.4	4.7899±0.0047 [53]	4.809	5.023	0.213	0.049	NL3 [52]
^{136}Xe	8.9	4.7964±0.0047 [53]	4.826	5.059	0.233	0.069	NL3 [52]

Finite impact parameter range

- Straight line geometry
- Integrated density within 1 interaction length ~0.18fm^2 at 2.4GeV/*c*

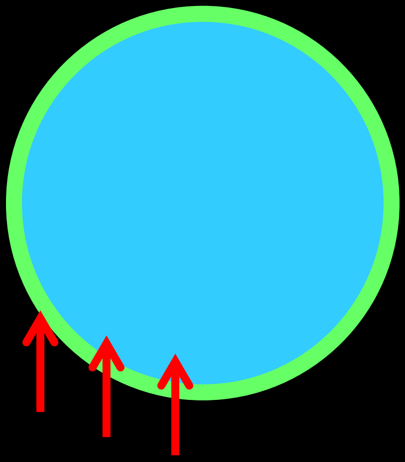

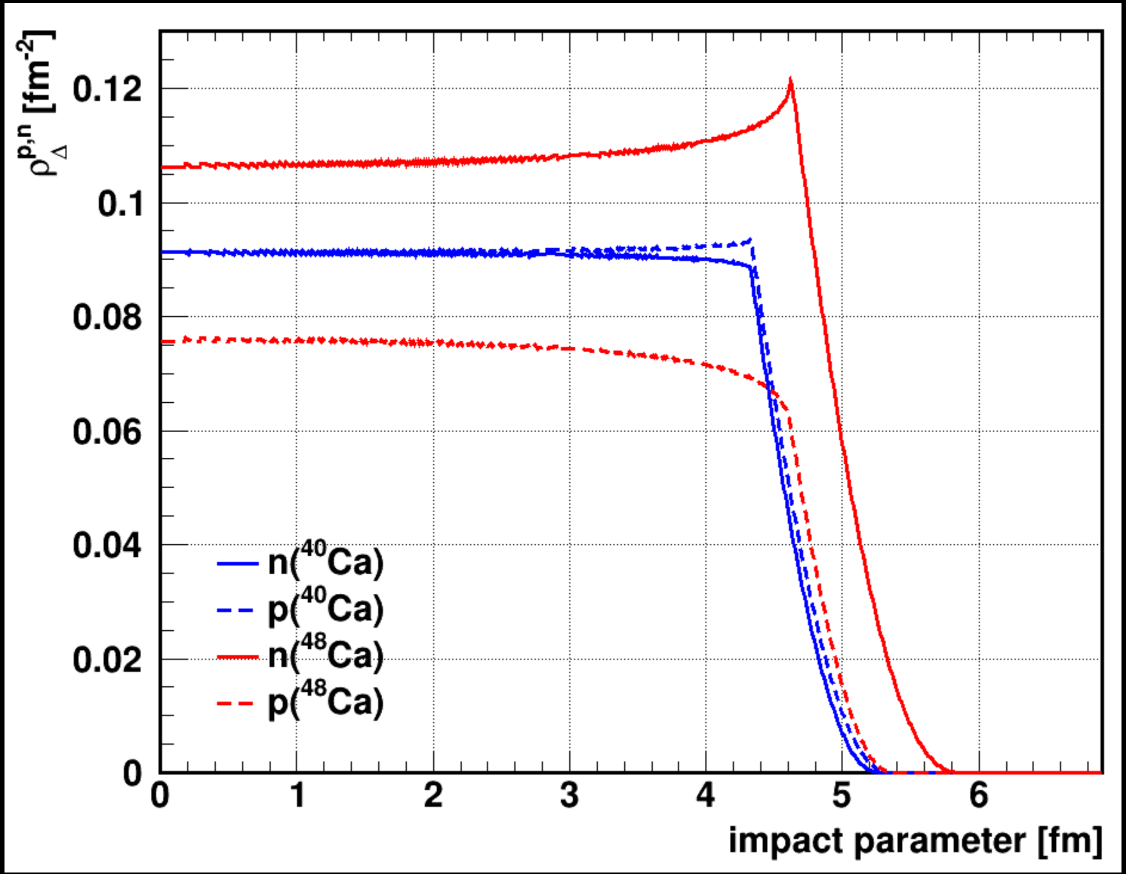

- Impact parameter averaged neutron-to-proton ratio: ^{40}Ca 0.97 and ^{48}Ca 1.65

Full transport calculations: GiBUU

target	RMF model	p($\overline{p}$) [GeV/c]	events [10^6]	$\Lambda\overline{\Lambda}$	$\Sigma^-\overline{\Lambda}$	double ratio GiBUU	double ratio Equation 9	double ratio ρ_Δ
^{20}Ne	NL3 [52]	1.7	99	7579	1629	—	—	—
^{22}Ne	NL3 [52]	1.7	98	6347	1965	1.440±0.054	1.115	1.328
^{20}Ne	NL3 [52]	2.4	167	32387	10870	—	—	—
^{22}Ne	NL3 [52]	2.4	171	29227	13297	1.356±0.021	1.100	1.309
^{40}Ca	NL1 [52]	2.4	415	76323	22880	—	—	—
^{48}Ca	NL1 [52]	2.4	450	66694	36074	1.799±0.018	1.224	1.703
^{40}Ca	NL3 [52]	2.4	415	74280	21827	—	—	—
^{48}Ca	NL3 [52]	2.4	450	61313	32391	1.798±0.019	1.207	1.705
^{40}Ca	NL3* [55]	2.4	415	78753	23438	—	—	—
^{48}Ca	NL3* [55]	2.4	450	64212	34523	1.807±0.018	1.210	1.707
^{40}Ca	Set I [56]	2.4	415	67000	17446	—	—	—
^{48}Ca	Set I [56]	2.4	450	57016	26042	1.754±0.020	1.129	1.691
^{58}Ni	NL3 [52]	2.4	100	16811	5230	—	—	—
^{64}Ni	NL3 [52]	2.4	108	14978	6534	1.402±0.030	1.113	1.358
^{129}Xe	NL3 [52]	2.4	109	13717	6238	—	—	—
^{130}Xe	NL3 [52]	2.4	109	13394	6225	1.022±0.022	1.001	1.036
^{131}Xe	NL3 [52]	2.4	109	13403	6379	1.047±0.023	1.018	1.050
^{132}Xe	NL3 [52]	2.4	109	13335	6556	1.081±0.023	1.026	1.084
^{134}Xe	NL3 [52]	2.4	109	12771	6656	1.146±0.025	1.043	1.134
^{136}Xe	NL3 [52]	2.4	109	12680	6739	1.169±0.025	1.062	1.184

BUU vs. Schematic model

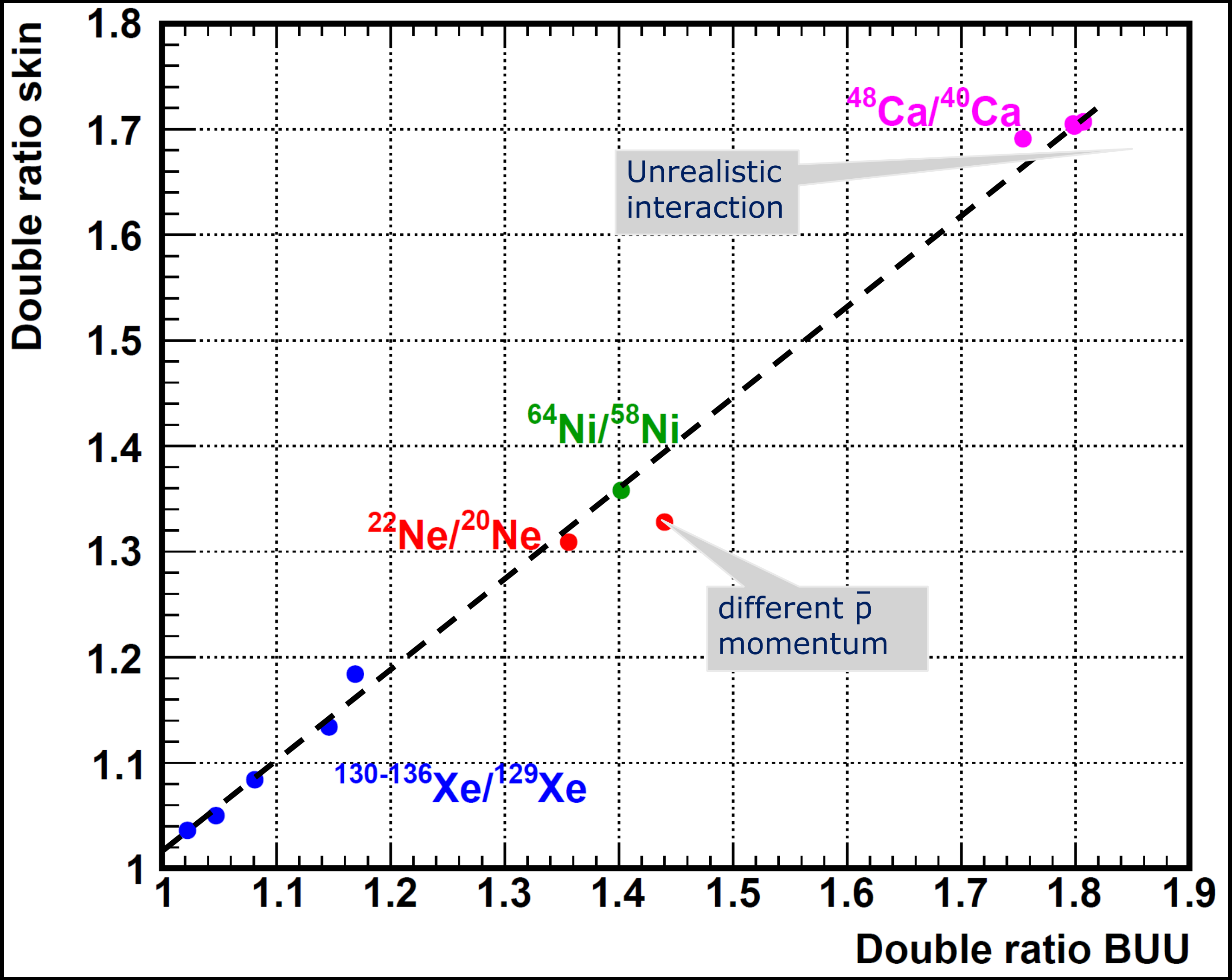

- Advantage of schematic model: explore sensitivity between neutron skin and double ratio

Sensitivity

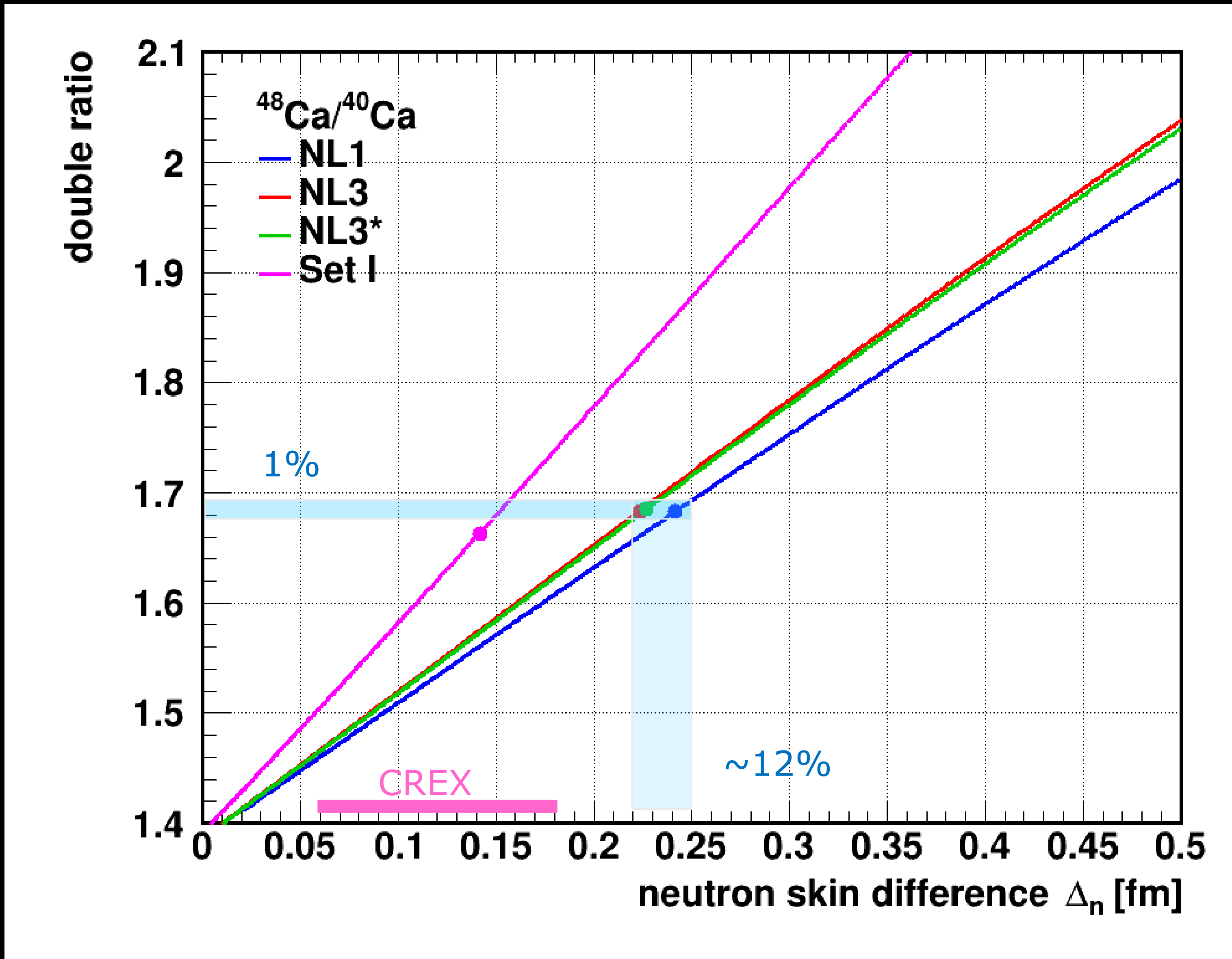

Experimental reqirements

- PANDA detector as reference
- Goal: 1% measurement of double ratio
- $2 \cdot 10^6$ interaction per second
- Reconstruction efficiency
  - Λ 30%
  - $\overline{\Lambda}$ 30%
  - Σ^- 3% (detection of n required!)
- S/B =73
- Statistical uncertainty limited by Σ^-
- Required time ~1 day at PANDA

- There are many interesting topics for energetic antiproton beams

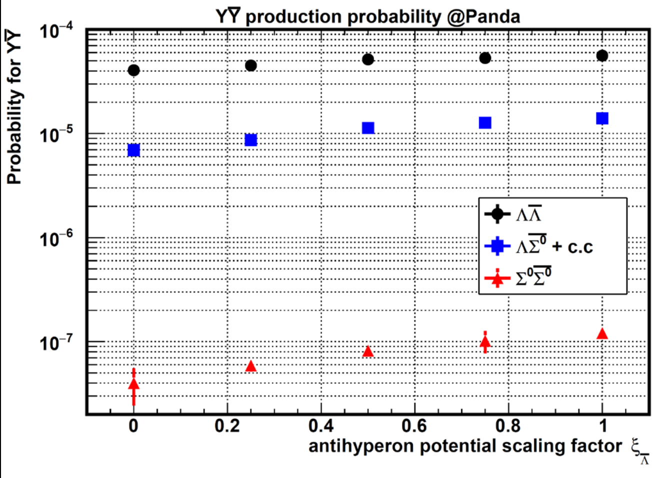

D16.2: Development of dedicated simulation and software tools for the measurement of antihyperons in nuclei.

Falk Schupp[1,§], Josef Pochodzalla[1,2]
representing the Networking activity THEIA (WP16) within STRONG-2020

[1] *Helmholtz Institute Mainz, Johannes Gutenberg University, 55099 Mainz, Germany*
[2] *Institute for Nuclear Physics, Johannes Gutenberg University, 55099 Mainz, Germany*

STRONG 2020
This project has received funding from the European Union's Horizon 2020 research and innovation programme under grant agreement No 824093.

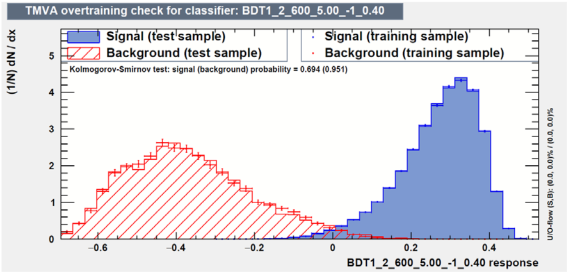

Figure 10: Output of the boosted decision tree (BDT) algorithm for background events (red histogram) and signal events (blue histogram).